Millimeter-Wave Radiometric Information Content Analysis for Venus Atmospheric Constituents

Enter authors here: N. Mathew [1], S. Sahoo[2], Renju R. [1] and C. Suresh Raju[1]

[1]Space Physics Laboratory (SPL) Vikram Sarabhai Space Centre (VSSC), ISRO, India.

[2]Electrical Engineering, Indian Institute of Technology Palakkad, India.

Corresponding author: Swaroop and Sahoo (swaroop@iitpkd.ac.in)

†Additional author notes should be indicated with symbols (for example, for current addresses).

Key Points:

- Millimeter and submillimeter frequency measurements of Venus mesosphere are prospective because they can measure several minor species
- Simulated brightness temperatures for 100-700 GHz have been analyzed to determine the frequency bands for estimation of various constituents concentration
- The sensitivity of measurements have been determined for the selection of measurement frequencies

This article has been accepted for publication and undergone full peer review but has not been through the copyediting, typesetting, pagination and proofreading process which may lead to differences between this version and the Version of Record. Please cite this article as doi: 10.1029/2019RS006913

Abstract

Various gaseous constituents present in Venus atmosphere have been detected and measured using in-situ and remote sensing instruments. However, the measurements of mesospheric constituents above the cloud level are still scarce and inadequate. This is because constituents above the cloud level have a low abundance and a high level of variability. However, millimeter and submillimeter (mm and sub-mm) frequencies can be used for Venus mesosphere measurements during prolonged Venusian day and night because several minor species in the upper atmosphere have emission/absorption bands in these frequencies owing to the rotational transitions. This study presents brightness temperatures and the corresponding sensitivity at the mm and sub-mm wave frequencies for a limb sounding radiometer. This will be useful in potential payload i.e., instrument design, frequency, bandwidth selection, satellite altitude as well as pointing accuracy determination for measurement above Venus clouds. For this study, a simulation based experiment has been performed and presented to determine the mm and sub-mm wave frequencies, optimum for estimation of concentration of water vapor, CO, CO_2, SO_2, HDO and HCl present in mesosphere. The simulations have been performed using a radiative transfer model Atmospheric Radiative Transfer Simulator. The mm and sub-mm wave measurement frequencies have been determined for both day and night time of Venus. It has been determined that 183, 380, 448, and 556 GHz frequencies are most suitable for water vapor measurements, 115, 230, and 345 GHz are optimum for CO measurements and 600, 621, and 690 GHz frequency measurements are sensitive for HCl detection.

1 Introduction

Venus has many similarities with planet Earth in terms of size, relative density, comparative surface gravity and distance from the Sun (Taylor et al., 2007). However, Venus atmospheric temperature, pressure and constituents profiles are significantly different from those of Earth. The atmospheric pressure at Venus surface is approximately ninety times that of Earth surface while the surface temperature is above 730 K (Williams, 2016). In addition to that, the presence of CO_2 dominated greenhouse atmosphere and thick sulphuric acid clouds in the altitude range of 40-60 km makes Venus atmosphere very different from that of earth. The presence of clouds does not permit the probing of the Venus surface and its atmosphere below the cloud base altitude using visible and infrared (VIS/IR) remote sensing. Thus, the Venus atmosphere has not been sampled continuously in terms of space, time as well as atmospheric composition and the associated variabilities are not estimated properly. Many missions have been sent to Venus to study its various constituents. These missions were either landers which made in-situ measurements or orbiters which made remote sensing measurements. They were the Mariner missions (Snyder, 1997, Chase et. al., 1963, Sonett, 1963), Pioneer Venus mission (Williams et. al., 1983) and Magellan mission launched by National Aeronautics and Space Administration (NASA) (Lyons et. al., 1995) while the Venera missions (Avduevsky et. al, 1968) were sent by the Soviet Union Space Program. The various atmospheric constituents of Venus have been studied and analyzed by these Venus Orbiter missions; the recently launched Venus Express (Titov et. al., 2006) by European Space Agency (ESA) and Akatsuki (Peralta et. al., 2017) by Japan Aerospace Exploration Agency (JAXA) being the latest missions. However, the concentration of many species and their isotopic ratios are not known with acceptable accuracy. Considerable uncertainty is associated with Venus mesospheric constituents, their concentration and the variability (Sandor et. al., 2005).

Based on the data from the Venus missions it has been determined that the main constituents of the atmosphere are carbon dioxide (Taylor and Grinspoon, 2009, Gilli et. al, 2009) with

abundance of 96.5% and N_2 (Taylor et al., 2018) with abundance of 3.5%. The abundance of carbon dioxide and N_2 is almost constant. There is significant amount of sulphur compounds, specifically gaseous H_2SO_4 and SO_2 (Taylor et al., 2018) while H_2O, CO and HCl are trace gases (Bézard et. al., 1990). The other constituent which is found in traces is HF, along with several isotopic ratios. The isotropic ratios include deuterium to hydrogen fraction which is more than a hundred times higher than on Earth (Fegley et al., 1997). All the trace gases including the noble gases Ar, Kr, Xe, and Ne are probably volcanic in origin. In addition to the above, water is also present on Venus as vapor in the atmosphere and the content does not exceed 100 ppm at any altitude and is bound with sulphuric acid in the cloud droplets. However, the total water abundance is significantly small in comparison to carbon dioxide and nitrogen (Marcq et al., 2018).

The runaway greenhouse effect, the direct and continuous interaction of solar winds with atmosphere induces large changes in the Venus upper atmospheric constituents as well as their distributions with altitude. The temperature and pressure above the Venus clouds altitude are closer to that of earth's lower atmosphere except the atmospheric constituents. Because of the varied distribution of the various constituents in the altitudinal domain, the scientific community is very interested in the detection of atmospheric constituents and the estimation of their populations. Most of the previous Venus missions were employing visible/IR based spectroscopic studies for atmosphere probing. However, there have been a few studies suggesting different species retrieval using millimeter/submillimeter wave radiometry at Venus mesospheric altitudes (Peralta et al., 2017). Millimeter (mm) and submillimeter (sub-mm) measurements of Venus mesosphere are very prospective because they can measure several minor species in the upper atmosphere (owing to the strong rotational transitions bands of the constituents).

The satellite based radiometric probing using the nadir viewing geometry has many limitations, in case of Venus. Some of them are: highly reflective acid clouds in the visible/IR spectral domain, very warm and thick lower atmosphere, large scattering by cloud particles in mm/submm wavelength domain, thermally brighter Venus surface and lower atmosphere, and limited atmospheric models available for employing radiative transfer based thermal emission computation. These limitations can be studied using simulation based experiment in the mm and sub-mm frequency band. Simulation based study has been performed using the Atmospheric Radiative Transfer Simulator (ARTS) model (Schreier et. al., 2014). The ARTS model gives the facility to simulate the brightness temperature (measurements) at specific satellite altitudes and for any given viewing geometry. The sensitivity of different frequencies at different altitudes can also be derived by the brightness temperatures simulated using ARTS, which is very much a primary information for the design of a radiometer. The ARTS simulations provide possible wide range of frequencies and optimized bands of frequencies to study maximum number of species considering the sensor availability at these frequencies.

Above the Venus cloud-top the atmospheric pressure is very low and volume mixing ratios (VMR) of many species are also very small. Thus, the brightness temperatures can be considerably low at ~50-100 K corresponding to constituents VMR in the range of 2-20 ppm. Therefore, a limb sounding technique has been chosen as the most viable viewing geometry. The limb viewing technique will measure the radiation from the atmospheric constituents (whose VMR are very small) with good vertical resolution while not being affected by comparatively warmer lower atmosphere and surface emissions.

The ARTS radiative transfer model is used to study the mm and sub-mm emission characteristics of different species such as H_2SO_4, H_2O, SO_2, CO and HCl in the Venus atmosphere above the clouds. This study is performed over a wide spectral region ranging from 100 to 700 GHz using limb viewing geometry. This wide spectral region (which includes natural resonant rotational absorption/emission frequency bands of various

constituents) is used for simulating brightness temperatures of these species at different altitudes from just above the acid cloud (60 km) to 90 km. These simulated brightness temperatures are the essential inputs for the selection of optimum range of frequency bands for designing the future mm/submm radiometers for Venus atmosphere studies. The rate of change of brightness temperatures (at frequencies of interest) with change in volume mixing ratio of the constituents have been determined which provides significant information for the selection of measurement frequencies and the performance of a measurement in concentration retrieval. Thus, this study provides quantitative analysis of the measurement frequencies, corresponding sensitivities and bands of operation.

The paper has been organized in in 8 Sections. This Section has given information about the concentrations of Venus atmospheric constituents and the various missions that have been sent to Venus. Section 2 discusses the spatial (altitude) distribution of various trace gases i.e., sulphuric acids, ozone, carbon monoxide, hydrogen chloride, sulphur dioxide and water vapor. Section 3 discusses the deployment strategy i.e., limb sounding geometry used for the simulation while Section 4 explains the radiative transfer simulator used for this study. The simulated brightness temperatures as well as the associated sensitivities are discussed in sections 5, 6 and 7, respectively. The summary and discussion is given in Section 8.

2 Major Trace Gases and their Proportion

The goal of the present study is to investigate the possibility of mm/submm (100-700 GHz) wave radiometry to detect various atmospheric constituents and determine the corresponding abundances using inversion of radiative transfer computations. So, the importance of major trace gases and their distribution in Venus atmosphere have been discussed in the next sub-sections.

2.1 Sulphuric Acid

The Venus cloud is made up of photochemically produced, micron-sized sulphuric acid droplets and its formation is the main feature of photochemistry (Krasnopolsky, 2015). Therefore, sulphuric acid cloud is one of the most important constituents of Venus atmosphere because of its impact on the radiative transfer and also on the region in Venus where large abundance of water exists. The formation of sulphuric acid takes place in the upper atmosphere, above the cloud tops. The atomic oxygen above the cloud top combines with SO_2 to produce SO_3, which again reacts with water vapor to form H_2SO_4. The atomic oxygen is formed by the dissociation of water and carbon dioxide by solar ultraviolet radiation. Sulphuric acid has a maximum abundance of 7.5 ppm at the lower cloud boundary of 47 km while the maximum abundance is 0.1 ppm at 53 km. These values have been determined theoretically and verified by observations performed by the VeRa radio occultation of Venus Express (Oschlisniok et. al., 2012).

2.2 Carbon monoxide (CO)

CO_2 dissociates into CO in the mesosphere using solar ultraviolet radiation (Taylor et al., 2018). The CO and O are transported to the nightside using atmospheric circulations (Vandaele et al., 2015), thus producing a significant variation in CO density with space. The presence of CO affects the abundance of various greenhouse gases. In addition to that, CO is a well-mixed gas and its measurement can be used to derive temperature profile of Venus mesosphere. Thus measurement of CO in Venus is of utmost importance and has to be done as accurately as possible. It has been estimated that the CO density has a lower limit of 200 ppm (de Pater and Lissauer, 2001), and has a VMR range of 350–1400 ppm (von Zahn et al., 1983). Solar occultation at Infrared (SOIR) aboard Venus Express (VEX) has been used to determine the CO density at 120 km between 700 and 40000 ppm, with a mean value of

approximately 3300 ppm (Vandaele et al., 2016). There is a possibility that the CO density decreases significantly from 70 km to 140 km by an order of 104 (Vandaele et al., 2016).

2.3 Hydrogen chloride (HCl)

Hydrogen chloride (HCl) forms in the Venus cloud (Iwagami, 2008, Hapke, 1972) and the estimation of HCl concentration would be a pointer to the formation and composition of the clouds. The mixing ratio of HCl has been estimated to be approximately 0.1 ppmv in the mesosphere (de Pater and Lissauer, 2001). This mixing ratio value has been found to be consistent with the measurements performed by solar occultation in the InfraRed (SOIR) on board VEX. The HCl values range was found to be 0.1 ± 0.03 ppm and 0.17±0.03 ppm for altitude range of 70–75 km (Bertaux et al., 2007).

2.4 Sulphur dioxide (SO_2)

SO_2 is an important constituent because of its role in forming sulphuric acid cloud. It has a high mixing ratio of approximately 150-200 ppm below the cloud (de Pater and Lissauer, 2001, von Zahn et al., 1983; Taylor et al., 2018, Pollack et. al., 1993), but decreases quickly inside the cloud region. The mixing ratio of SO_2 reduces to almost 0.1 ppm at 70 km, due to conversion from SO_2 to H_2SO_4 (von Zahn et al., 1983). SO_2 above the cloud top was measured by the ultraviolet spectrometer Spectroscopy for Investigation of Characteristics of the Atmosphere of Venus (SPICAV) on VEX. The values of mixing ratio are approximately 0.1–0.2 ppm (Marcq et al., 2013). According to (Krasnopolsky, 2010), the mixing ratio stays constant up to around 110 km, before it decreases to around 60 ppb at 130 km.

2.5 Water Vapor

The water in the oceans of Venus evaporated due to which Venus became a very dry planetary body due to the runaway greenhouse effect. In this process the CO_2 stored in the ocean beds was liberated and the Venus atmosphere became CO_2 dominant. The present active volcanism is the major player for not only for the resurfacing of the Venus solid body but also the supplier for constituents required for the formation of sulphuric acid cloud. Water vapor abundance can be used for studying the evolution of Venus and for the study of formation of sulphuric acid cloud in Venus (Bezard, 2009). In addition to that, water vapor species can have H and D whose ratio can also be used for determining the evolution of Venus. This analysis will also determine the relative escape of each of the species of water from Venus. The in-situ analysis of Venus atmosphere based on Venera 4 data had already shown that water vapor is a minor constituent of the Venus atmosphere (Avduevsky et. al, 1968). The measurement by infrared imaging spectrometer (IRIS) a ground-based Anglo-Australian telescope (Meadows, 1996) and Visible and Infrared Thermal Imaging Spectrometer (VIRTIS) abroad Venus Express spacecraft (Bezard, 2009) have shown that water vapor mixing ratio from surface to the lower cloud level 30–40 km are consistent with the 30 ± 10 ppm abundance (where ppm is parts per million by volume). However, the microwave and IR observations of water vapor in the mesosphere and low thermosphere (70–120 km) are characterized by a lower mixing ratio of 0–5 ppm with about constant vertical distribution (Moroz et al., 1990; Koukouli et al., 2005). These studies have proved that there is significant variation in the distribution of water vapor in the Venus atmosphere above the cloud layer and the uncertainty could be 9 ppmv in horizontal distribution of water vapor as well as the diurnal variation. There is also a significant variation in water vapor on a yearly basis. Despite the numerous measurements, the mesospheric abundances measured in various experiments varied from 0 to 100 ppm. This variation is clearly seen in Figure 1.

The above discussion indicates that various constituents have concentration less than 10 ppm in the mesosphere and have a high amount of variability. Therefore, it is important to

determine the constituents and their spatial and temporal (daily and yearly) variability. This simulation based study has been performed with various mm/sub-mm wave channels for limb sounding radiometer. The next sections describe the deployment strategy of the radiometer and simulator to be used, frequency determination method and the simulated brightness temperatures for frequency range 100 to 700 GHz. The simulated brightness temperatures will be analyzed for sensitivity of the frequencies considered for the study.

3 Geometry of Measurement

There are various measurement strategies that have been used for remote sensing of planets from orbiters: primarily nadir viewing, limb viewing and radio occultation.
The brightness temperature for nadir viewing radiometer is calculated as (Gordy., 1993)

$$T_{Bnadir} = \Upsilon(\varepsilon\, T_s) + \Upsilon(1-\varepsilon)T_d + T_u \quad (1)$$

where Υ is the transmittance, ε is emissivity of the surface, T_s is temperature of the surface, T_d is down-welling brightness temperature and T_u is the upwelling brightness temperature. Transmittance is given by $\Upsilon = e^{-\tau}$where τ is the opacity (optical depth) of the medium and is dependent on the absorption coefficients of the medium. Nadir viewing, orbiter based radiometer in Venus atmosphere would be viewing a scene with physical temperature in the range of ~740 K. The brightness temperatures measured will be approximately, 500-600 K but the brightness temperature of the constituents of interest will be considerably low at 50-100 K. This is because the constituents will have a VMR in the range of 2-20 ppm. Therefore, a limb sounding technique has been chosen for the study where the technique will measure the radiation from the atmosphere with good vertical resolution but will not be affected by surface emissions (hot thermal background of Venus atmosphere). The brightness temperature for limb viewing radiometer will be calculated as (Janssen., 1993)

$$T_{BLIMB} = \Upsilon(T_{3K}) + T_u \quad (2)$$

where T_{3K} is the cosmic background temperature.
Using limb viewing technique, the mesospheric constituents for altitude range of 65-90 km need to be measured. A simulation based study has been performed assuming an orbiter altitude of approximately 450 km above ground surface and the zenith angles to be above 70-73^o. The position of the orbiter with respect to Venus is shown in Figure 2. Thus the radiometer ray passes through the mesosphere and the altitude of the ray can be varied using a scanning technique so as to cover 65-90 km.

4 Radiative Transfer Equation Model for Venus

Atmospheric radiative transfer simulator (ARTS) – version 2.2 (Buehler. et. al., 2018), the planetary toolbox has been used to simulate the brightness temperatures for the limb viewing radiometer on the orbiter. ARTS – version 2.2, the planetary toolbox has been developed with the main goal of simulating the brightness temperatures for various planets at a range of frequencies (upto 3 THz). The simulator also uses various viewing (occultation, limb and nadir) angles and distribution geometries (i.e., 1-D, 2-D and 3-D). The ARTS was initially developed for Earth and has been modified for Mars, Venus, and Jupiter. ARTS 2.2 simulator considers the atmospheric constituents N_2, O_2, H_2O, CO_2, H_2, and He as foreign broadening species. The line broadening of another planet due to basic atmospheric composition can be handled by using the concept of foreign broadening coefficient for a standard air mixture. The gases in the atmosphere have been chosen taking into consideration the most abundant and trace constituents in Venus, Earth, Mars, and Jupiter atmospheres. The model has sensor related information due to which efficient weighting of monochromatic pencil beam radiances can be performed.

5 Simulated Brightness Temperatures for Venus Atmospheric Constituents

Brightness temperatures were computed using ARTS simulator for various atmospheric constituents of Venus and for a range of frequencies (100-700 GHz). The various atmospheric constituents used for this study are water vapor, CO, HDO, SO_2 and HCl. The details of the brightness temperatures computed and the associated variability are discussed in the following subsections.

5.1 Water Vapor

Brightness temperatures have been computed for frequency range of 150-190 GHz using water vapor profile as the constituent for limb viewing geometry. For the simulation, water vapor and temperature profiles above the cloud top and in the mesosphere have been used as inputs to ARTS. The profiles for night time are shown in Figure 3 where the water vapor VMR is shown to vary from 30 ppmv to 3 ppmv for an altitude range of 20 to 100 km while the temperature changes from 600 to 200 K for the same altitude range. The simulated brightness temperatures for altitude range of 40-75 km with an increment of 5 km are shown in Figure 4. The brightness temperatures for altitudes 40 to 60 km are approximately 260-270 K and show no variation with frequency of measurement. This is because of contributions to brightness temperatures from the surface of thick clouds.

It is observed that the brightness temperatures for 65, 70 and 75 km are in the range of 200-250 K, 100-150 K and 10-50 K, respectively. Thus, as the altitude increases the brightness temperatures decrease but the sensitivity of the frequencies to water vapor distribution improves. This improvement in sensitivities of frequencies is observed at 160-165 GHz, 176 GHz and 182-186 GHz for altitudes of 65, 70 and 75 km.

5.2 H_2O, CO, HDO, SO_2 and HCl

A comprehensive study of the simulated brightness temperatures from H_2O, CO, HDO, SO_2 and HCl present above the cloud top and in the mesosphere has been performed. The sample profiles of CO, H_2O and SO_2 used for this simulation are shown in Figure 5. The profiles show that carbon monoxide VMR is less than 1 ppmv below 100 km and the proportion of carbon monoxide starts increasing above 100 km. The concentration of SO_2 shows an increasing trend above 20 km till 40 km and then decreases. The simulated brightness temperatures for 100-350, 320-350 and 100-700 GHz ranges are shown in Figure 6 to Figure 8.

Analysis of the results in Figure 6 show that the values of brightness temperature peaks vary from 100 to 250 K for 60 km, 50-200 K for 65 km, 30-150 K for 70 km and 10-100 K for 75 km. However, the brightness temperatures other than the peaks remain below 25 K for all altitudes and for all frequencies.

The various peaks at 115 GHz, 183 GHz, 226 GHz, 230 GHz, 335 GHz, 345 GHz and 346 GHz in the simulated brightness temperatures correspond to CO, H_2O, HDO, CO, HDO, CO and SO_2 (also the rotational lines for the constituents), respectively. These frequencies have higher associated opacity values contributing to the higher brightness temperatures. However, the opacities vary with the strength of the rotational frequency lines resulting in varying values of the peaks. The brightness temperatures for all frequencies reduce as the altitude increases and this corresponds to reduction in the abundance of the constituents. An important observation is the varying sensitivity of frequencies neighboring (window frequencies) to those of the peaks. This variation can be used for retrieval of the constituents' profiles. Therefore, the frequencies corresponding to the peaks can be used for determining

low concentrations at high altitudes while the frequencies further away but still sensitive to the constituents can be used for determining high concentration values.
The simulated brightness temperatures from 320 to 350 GHz for altitude range of 60-90 km are presented in Figure 7 to analyze the emission for CO, SO_2 and H_2O. It can be observed that the brightness temperatures for 60-65 km are higher than 200 K and show very limited frequency variation. Thus, they show saturation characteristics and no variation with change in frequency. The frequency based variation in brightness temperatures become obvious with increase in altitude which in turn corresponds to reduction in proportion of constituents. Thus, it can be observed that the measurement frequencies above 320 GHz, are sensitive to HDO (335 GHz), CO (345 GHz) and SO_2 (346 GHz) and can be used for detecting their sparse quantities even at altitudes of 85 km. The frequencies are also the rotational absorption lines for the constituents.

A comprehensive analysis was performed to simulate brightness temperatures for a frequency range of 100-700 GHz and the results are shown in Figure 8 for altitudes of 60-75 km. The brightness temperatures at 60 and 65 km are significantly higher than those at 70 and 75 km and the peaks for 60-65 km are higher by more than 50 K in comparison to the peaks at 70-75 km. It can be seen that the peak values keep on increasing as the frequency of measurements increases. The brightness temperatures for 60-70 km for frequency range of 100-350 GHz are lower than those between 400-700 GHz. The brightness temperature peaks for frequency range of 450-700 GHz are similar for all altitudes and are sensitive to traces of the constituents. Therefore, these frequencies are essential to get signatures of minor species existing in the higher altitudes in the limb viewing geometry. Thus, frequency range of 100-350 GHz can be used for high concentration constituents estimation while the 450-700 GHz can be used for low concentration constituents estimation. The peaks in the frequency range of 100-350 GHz and 450-700 GHz have comparatively different associated opacity (hence transmittance) values but the opacity values for peaks in 100-350 GHz are less than those for 450-700 GHz. The strength of the absorption lines in the 450-700 GHz range are higher than those in the 100-350 GHz range. Thus, the brightness temperature values keep on increasing with frequency for the same altitude.

6 Selection of Measurement Frequencies

Based on the analysis of the brightness temperatures for frequencies between 100-700 GHz (Figure 6, Figure 7 and Figure 8), it has been observed that particular discrete frequency measurements are most prominently sensitive to the constituents of interest in terms of detection. It is also seen that the higher frequencies (above 400 GHz) are very sensitive to low concentration of constituents but saturate as the concentration increases. However, the low frequencies (below 400 GHz) are sensitive to wider range of concentrations and hence can be used for retrieval of higher concentration as well as altitude profile. The frequencies which will be useful for measuring the particular constituents are shown in Table 1.
The frequency channels 115 and 230 GHz are sensitive to CO while multiple measurement frequencies ranging from 183 to 556 GHz are sensitive to water vapor. In addition to that, SO_2 can be measured by 346 GHz channel while HCl can be measured by frequency channels at 600, 621 and 690 GHz.

6.1 Water Vapor

Figure 8 shows that frequencies 160-165, 183-187, 380, 448 and 556 GHz have a significant sensitivity to water vapor. It is observed that the water vapor sensitive frequency measurements higher than 183 GHz have brightness temperatures of approximately 180 K (and higher) while 183 GHz shows a lower brightness temperature of approximately 15 K for

VMR of 1-2 ppmv (corresponds to altitude 75 km from Figure 5). The water vapor sensitive frequencies higher than 183 GHz have brightness temperatures of 250 K for a VMR of 10-15 ppmv (corresponds to altitude 60 km from Figure 5). Thus, the sensitivity for each of the frequency measurements is different and therefore better suited for measuring varying quantities of water vapor. The varying sensitivity of the channels show that frequencies near 183 GHz are good for measurement of water vapor profiles with concentration in the range of 5-10 ppmv while 380, 448 and 556 GHz are good for measurement of very small quantities of water vapor in the range of 1-2 ppmv. Therefore, combinations of water vapor measurement frequencies can be used for retrieval of vertical distribution of water vapor for altitudes at/above 65 km. In addition, pressure broadened for 380, 448 and 556 GHz can be also used for water vapor profile retrieval. It is important to know that 183, 380, 448 and 556 GHz are the resonance frequencies for water vapor (Rosenkranz, 1998, Prigent, 2006).

6.2 Carbon Monoxide

The simulated measurements in Figure 8 for 115 and 230 GHz show values of approximately 25 K while measurements at 345 GHz have values of approximately 50 K at 75 km altitude. Thus, the highly sensitive, 345 GHz channel can be used for detecting very small amounts of CO. In addition to that, the brightness temperatures for 115, 230 and 345 GHz show altitude based variation. Since, CO is a well-mixed gas in Venus atmosphere, it can be used for temperature profile retrieval.

6.3 Sulphur Dioxide

The simulated measurements in Figure 8 show that SO_2 brightness temperature peaks at 346 GHz. For this constituent, pressure broadening has to be used for determining profiles of SO_2. Thus, a combination of 346 GHz and the neighboring frequencies can be used for measurement of profiles.

6.4 HDO

The brightness temperatures from the simulations show that HDO can be measured using 226 and 335 GHz where 335 GHz measurement is more sensitive than 226 GHz. So, both can be used for determining varying level of HDO.

6.5 Hydrogen Chloride

The simulations have shown that HCl can be measured using multiple frequencies i.e., 600, 621 and 690 GHz, which are in the higher part of submm spectra. All the three frequencies show varying amount of sensitivity to HCl but they have similar brightness temperatures of 250 K at 60 km. In addition to that 621 and 690 GHz show varying brightness temperatures for different altitude but 600 GHz shows the same brightness temperatures for all altitudes. Thus, 621 and 690 GHz are optimum for profile retrieval using pressure broadening as can be observed from the brightness temperature curves in Figure 8 while 600 GHz is optimum for measuring very small amounts of HCl because of its highest sensitivity.

In instrument design an important analysis is to determine the range of frequencies which will be optimum for various constituent measurement and estimation. The optimum frequency range is 100-400 GHz and the corresponding constituents of interest in that band that can be detected and measured are shown in Table 2.

7 Sensitivity Analysis of Frequency Measurement for H_2O and SO_2

The various frequencies selected for water vapor and sulphur dioxide measurements have varying sensitivities for concentrations of water vapor and sulphur dioxide. These varying

sensitivities of the frequency measurements needs to be analyzed and are discussed in this section.

7.1 Water Vapor

The frequencies 183, 380, 448 and 556 GHz have varying rates of change of brightness temperatures for varying abundances of water vapor as discussed here and shown in Figure 9. The rate of change of brightness temperatures has been presented for a VMR range of 3-10 ppmv. The brightness temperatures for 380, 448 and 556 GHz (~165, 185 and 200 K, respectively) are higher than that of 183 GHz (15 K) at 1 ppmv. 183 and 380 GHz have a higher rate of change of brightness temperatures than 448 and 556 GHz for the VMR range under consideration. In addition, all the sensitvities show decreasing trend of rate of change of brightness temperature with increase in VMR. Thus, for VMR values less than 2 ppmv, 380, 448 and 556 GHz can be used for detecting and estimating concentrations while for ppmv values higher than 3 ppmv, 183 and 380 GHz can be used for estimation of VMR values.

7.2 Sulphur Dioxide

The measurement frequency sensitive to sulphur dioxide as per table 1 is 346 GHz and the rate of change of brightness temperatures with change in VMR of sulphur dioxide is shown in Figure 10. The rate of change is highest at 5 ppmv and starts decreasing as the concentration of sulphur dioxide increases.

8 Summary and Discussion

Hot surface temperature, warmer lower atmosphere and about 20 km or more thick sulphuric acid clouds are the major limiting factors of nadir viewing satellite measurements at mmwave and submmwave for the atmosphere studies. The atmosphere in this region is also very thin and VMR of many species are very small. Therefore, limb viewing radiometer on a satellite provides a good opportunity to measure mesospheric constituents' concentrations and their vertical distribution with good vertical resolution. The strong absorption/emission bands of many species in the mm/submm spectral region are another added advantage which permit the quantification of very sparsely distributed species. As a result, mmwave/submmwave frequency band is a potential range of spectrum to study Venus atmosphere. This study demonstrates the optimum frequency range at which one can analyze the most number of atmospheric constituents in the Venus mesosphere from the top of the clouds. This will be a primary input for designing an orbiter based limb viewing radiometer.

A simulation based study has been performed to determine a set of mm/submm frequencies suitable to detect different mesospheric constituents in Venus atmosphere and estimate their concentration from limb pointing radiometer. This study also determines a frequency band that maximizes the number of species detectable using the radiometric sounder. For this study, the brightness temperatures for limb geometry have been simulated using ARTS planetary model over a wide range of frequencies and for the mesospheric region of Venus atmosphere above the cloud-top. The sensitivity of different frequencies to various species and altitudes has also been estimated, which can be used as primary information for the design of a radiometer.

The simulation based study has demonstrated that trace gases considered in this paper can be detected and their concentration estimated using frequencies from 100 to 700 GHz. Water

vapor has the most number of sensitive frequencies for detection and estimation of concentration. In addition to that, frequencies neighboring to water vapor absorption line (183, 380, 448 and 556 GHz) can be used for profile estimation. It has also been determined that the rate of changes of brightness temperatures with VMR for 183 and 380 GHz are higher than those of 448 and 556 GHz for VMR range 2-10 ppmv. However, this rate shows decreasing trend for all frequencies.

As part of the study, it has been demonstrated that carbon monoxide concentration can be estimated using the CO rotation lines at 115, 230 and 345 GHz. 115 and 230 GHz show lower brightness temperatures than 345 GHz at 75 km. As the altitude decreases, the brightness temperatures increases, however measurements at 345 GHz saturate at lower altitudes while those measurements at 115 and 230 GHz do not. Therefore, 115 and 230 GHz are suitable for retrieving high concentration of CO while 345 GHz can be used to estimated low values of CO concentration. The combination of the three frequencies can be used for profile retrieval.

On the other hand, SO_2 is detectable only at 346 GHz which has a sensitivity of 40 K/ppmv at 5 ppmv and decreases as the VMR value increases. HDO can be measured at two frequencies at 226 and 335 GHz and pressure broadening can be used for measuring altitude distribution of HDO. While, the measurement frequencies selected for HCl are 600, 621 and 690 GHz. HCl detection frequencies can also be used for profile retrieval using pressure broadening.

In addition to that, the extent of use of mm and sub-mm wave radiometer for the detection of various constituents' has been analyzed. It can be observed from various simulations based results in Figure 4, Figure 6, Figure 7 and Figure 8 that the constituents concentration can be retrieved above an altitude of 60 km. Measurements below this altitude are difficult because of higher opacity due to higher atmospheric concentration, thick cloud cover and ambient temperatures. It is also observed that the brightness temperatures increase significantly with frequency above 450 GHz.

Acknowledgement

The brightness temperature simulations have been performed using the radiative transfer model ARTS and the associated atmospheric profiles. The data can be found in the archive Zenodo: https://zenodo.org/record/3545952#.XfBouegzbIU

References

Avduevsky, V. S., Marov, M. Y., Rozhdestvensky, M. K. (1968). Model of the Atmosphere of the Planet Venus Based on Results of Measurements made by the Soviet Automatic Interplanetary Station Venera 4. *J. Atmos. Sci.*, 25, 537-545. https://doi.org/10.1175/1520-0469(1968)025<0537:MOTAOT>2.0.CO;2.

Bézard, B., De Bergh, C., Crisp, D., and Maillard, J. P. (1990). The deep atmosphere of Venus revealed by high-resolution nightside spectra. *Nature*, 345, 508– 511.

Bézard, B., Tsang, C. C. C., Carlson, R. W., Piccioni, G., Marcq, E., Drossart, P. (2009). Water vapor abundance near the surface of Venus from Venus Express/VIRTIS observations. *J. Geophys. Res.*,114(E5), 1-12. https://doi.org/10.1029/2008JE003251.

Buehler, S. A., Mendrok, J., Eriksson, P., Perrin, A., Larsson, R., Lemke, O. (2018). ARTS, the Atmospheric Radiative Transfer Simulator – version 2.2, the planetary toolbox edition. *Geosci. Model Dev*, 11(4), 1537–1556. doi: 10.5194/gmd-11-1537-2018.

Chase, S. C., Kaplan, L. D., Neugebauer, G. (1963). The Mariner 2 infrared radiometer experiment. *J. Geophys. Res.* 68 (22), 6157-6169. doi: https://doi.org/10.1029/JZ068i022p06157.

Cottini, V., Ignatiev, N. I., Piccioni, G., Drossart, P., Grassi, D., Markiewicz, W. J. (2012). Water vapor near the cloud tops of Venus from Venus Express/VIRTIS dayside data. *Icarus*, 217(2), 561-569. https://doi.org/10.1016/j.icarus.2011.06.018.

De Pater, I., Lissauer, J. (2001). *Planetary Sciences (1st ed.)*, Cambridge University Press.

Fedorova, A. et al., (2008). HDO and H2O vertical distributions and isotopic ratio in the Venus mesosphere by solar occultation at infrared spectrometer on board Venus Express. *J. Geophys. Res.* 113, E00B22. https://doi.org/10.1029/2008JE003146

Gilli, G., López-Valverde, M. A., Drossart, P., Piccioni, G., Erard, S., Cardesín Moinelo, A. (2009). Limb observations of CO2 and CO non-LTE emissions in the Venus atmosphere. *J. Geophys. Res.* 114(E5), 1-19. doi: 10.1029/2008JE003112.

Gordy, N. C., (1993). Remote sensing of the atmosphere from satellites using microwave radiometry, In Janssen, M. A., *Atmospheric Remote Sensing by Microwave Radiometry*, (pp. 1-35) New York, NY, USA: Wiley-Interscience.

Gurwell, M.A., Melnick, G.J., Tolls, V., Bergin, E.A., Patten, B.M., (2007). SWAS observations of water vapor in the Venus mesosphere. *Icarus*, 188(2), 288–304. https://doi.org/10.1016/j.icarus.2006.12.004.

Hapke, B. (1972). Venus Clouds: A dirty hydrochloric acid model. *Science*, 175 (4023), 748-751.

Iwagami, N., et.al. (2008). Hemispheric distributions of HCl above and below the Venus' clouds by ground-based 1.7 μm spectroscopy. *Planetary and Space Science*, 56 (10), 1424-1434. https://doi.org/10.1016/j.pss.2008.05.009

Krasnopolsky, V.A. (2007). Chemical kinetic model for the lower atmosphere of Venus. *Icarus*, 191(1), 25–37. https://doi.org/10.1016/j.icarus.2007.04.028.

Krasnopolsky, V. A. (2010). Venus night airglow: Ground-based detection of OH, observations of O2 emissions, and photochemical model, *Icarus*, 207(1), 17-27. doi:10.1016/j.icarus.2009.10.019.

Krasnopolsky, V. A. (2012). A photochemical model for the Venus atmosphere at 47–112 km, *Icarus*, 218(1), 17-27. doi:10.1016/j.icarus.2011.11.012.

Krasnopolsky, V. A. (2015). Vertical profiles of H2O, H2SO4, and sulfuric acid concentration at 45–75km on Venus. *Icarus*, 252, 327–333. doi:10.1016/j.icarus.2015.01.024.

Koukouli, M. E., Irwin, P. G. J., Taylor, F. W. (2005). Water abundance in Venus middle atmosphere from Pioneer Venus OIR and Venera 15 FTS measurements, *Icarus*, 173, 84–99. doi:10.1016/j.icarus.2004.08.023.

Lyons, D. T., Saunders, R. S., Griffith, D. G. (1995). The Magellan Venus mapping mission: Aerobraking operations. *Acta Astronautica*, 35 (9-11), 669-676. https://doi.org/10.1016/0094-5765(95)00032-U.

Marcq, E., Bertaux, J. L., Montmessin, F., Belyaev, D. (2013). Variations of sulphur dioxide at the cloud top of Venus's dynamic atmosphere. *Nat. Geosci.*, 6 (1), 25–28. https://doi.org/10.1038/ngeo1650.

Marcq, E., Mills, F.P., Parkinson, C. D., Vandaele, A.C. (2018). Composition and chemistry of the neutral atmosphere. *Space Sci. Rev.*, 214(10), 1-55. Doi:10.1007/s11214-017-0438-5.

Meadows, V. S., Crisp, D. (1996). Ground-based near-infrared observations of the Venus nightside: The thermal structure and water abundance near the surface. *J. Geophys. Res.*, 101(E2), 4595-4622. doi: 10.1029/95JE03567.

Montmessin, F., Bertaux, J. L., Lefèvre, F., Marcq, E., Belyaev, D., Gérard, J. C., et al. (2011). A layer of ozone detected in the nightside upper atmosphere of Venus. *Icarus*, 216(1), 82–85. doi:10.1016/j.icarus.2011.08.010.

Moroz, V. I., Spankuchb, D., Titova, D. V., Schaferc, K., Dyachkova, A. V., Dohlerb, W., Zasovaa, L. V., Oerteld, D., Linkina, V. M., Nopirakowskid, J. (1990). Water vapor and sulfur dioxide abundances at the Venus cloud tops from the Venera 15 infrared spectrometry data. *Adv. Space Res.*, 10, 77–81. https://doi.org/10.1016/0273-1177(90)90168-Y.

Oschlisniok, J. et al., (2012). Microwave absorptivity by sulfuric acid in the Venus atmosphere: First results from the Venus Express Radio Science experiment VeRa. *Icarus*, 221, 940–948. https://doi.org/10.1016/j.icarus.2012.09.029

Peralta, J., Lee, Y. J., McGouldrick, K., Sagawa, H., Sánchez-Lavega, A., Imamura, T., Widemann, T., Nakamura, M. (2017). Overview of useful spectral regions for Venus: An update to encourage observations complementary to the Akatsuki mission. *Icarus*, 288, 235–239. https://doi.org/10.1016/j.icarus.2017.01.027

Pollack, J. B., Dalton, J. B., Grinspoon, D., Wattson, R. B., Freedman, R., Crisp, D., et al. (1993). Near-infrared light from Venus' nightside: A spectroscopic analysis. *Icarus*, 103, 1–42. https://doi.org/10.1006/icar.1993.1055.

Prigent, C., Pardo, J. R., Rossow, W. B. (2006). Comparisons of the millimeter and submillimeter bands for atmospheric temperature and water vapor soundings for clear and cloudy skies. *J. of Appl. Meteor. and Clim.*, 45, 1622-1633. https://doi.org/10.1175/JAM2438.1.

Rosenkranz, P. W. (1998). Water vapor microwave continuum absorption: A comparison of measurements and models. *Radio Science*, 33(4), 919-928.

Sandor, B. J., Clancy, R. T. (2005). Water vapor variations in the Venus mesosphere from microwave spectra. *Icarus*, 177, 129–143. doi:10.1016/j.icarus.2005.03.020.

Schreier, F., Gimeno García, S., Hedelt, P., Hess, M., Mendrok, J., Vasquez, M., & Xu, J. (2014). GARLIC — A general purpose atmospheric radiative transfer line-by-line infrared-microwave code: Implementation and evaluation. *Journal of Quantitative Spectroscopy and Radiative Transfer*, 137, 29–50. doi:10.1016/j.jqsrt.2013.11.018.

Snyder C.W. (1997). *Mariner missions. In: Encyclopedia of Planetary Science.* Encyclopedia of Earth Science. Springer, Dordrecht.

Sonett, C. P., (1963). A summary review of the scientific findings of the Mariner Venus mission. *Space Science Reviews*, 2 (6), 751-777. doi: https://doi.org/10.1007/BF00208814.

Taylor, F.W., Svedhem, H., Titov, D. (2007). Venus Express and terrestrial planet climatology, in L.W. Esposito, E.R. Stofan, T.E. Cravens. *Geophysical Monograph Series*, (vol. 176, pp. 157-170), Washington, DC: American Geophysical Union.

Taylor, F., Grinspoon, D. (2009). Climate evolution of Venus. *J. Geophys. Res.*, 114(E00B40), 1-22. doi:10.1029/2008JE003316.

Taylor, F.W., Svedhem, H. and Head, J. W. (2018). Venus: The Atmosphere, Climate, Surface, Interior and Near-Space Environment of an Earth-Like Planet. *Space Science Rev.*, 214(35), 1-36. doi: 10.1007/s11214-018-0467-8.

Titov, D. V., Svedhem, H., McCoy, D., Lebreton, J. P., Barabash, S., Bertaux, J. L. (2006). Venus Express: Scientific goals, instrumentation, and scenario of the mission. *Cosmic Research*, 44(4), 334-348. https://doi.org/10.1134/S0010952506040071.

Vandaele, A.C., Mahieux, A., Robert, S., Drummond, R., Wilquet, V., Bertaux, J. L. (2015). Carbon monoxide short term variability observed on Venus with SOIR/VEX. *Planet. Space Sci.* 113–114, 237–255. doi:10.1016/j.pss.2014.12.012.

Vandaele, A. C., Chamberlain, S., Mahieux, A., Ristic, B., Robert, S., Thomas, I., et. al. (2016). Contribution from SOIR/VEX to the updated venus international reference atmosphere (VIRA). *Adv. Space Res.*, 57 (1), 443–458. http://dx.doi.org/10.1016/j.asr.2015.08.012.

Van den Berg, M. L., Falkner P., Atzei A. C., and Peacock A. (2006). Venus microsat explorer programme, an ESA technology reference study. *Acta Astronaut* 59, 593–597. https://doi.org/10.1016/j.actaastro.2005.07.006

Von Zahn, U., Kumar, S., Niemann, H., Prinn, R. (1983). *Composition of the Venus atmosphere (1st ed.)*. Tucson, AZ, University of Arizona Press.

Waters, J. R. (1993). Microwave limb sounding, In Janssen, M. A. *Atmospheric Remote Sensing by Microwave Radiometry*, (pp. 1-35) New York, NY, USA: Wiley-Interscience.

Williams, B.G., Mottinger, N. A., Panagiotacopulos, N. D. (1983). Venus gravity field: Pioneer Venus orbiter navigation results. *Icarus*, 56(3), 578-589. https://doi.org/10.1016/0019-1035(83)90175-6.

Williams, D. R., 2016. Venus fact sheet. Retrieved June 23, 2019, https://nssdc.gsfc.nasa.gov/planetary/factsheet /venusfact.html.

Zhang, X., Liang, M. C., Mills, F. P., Belyaev, D. A., Yung, Y. L., (2012). Sulfur chemistry in the middle atmosphere of Venus. *Icarus*, 217(2), 714-739. https://doi.org/10.1016/j.icarus.2011.06.016.

Table 1. *Frequencies selected for various constituents*

Venus Atmospheric Constituent	**Frequencies (GHz)**
CO	115, 230, 345
H_2O	183, 380, 448, 556
SO_2	346
HDO	226, 335
HCl	600, 621, 690

Table 2. *The frequency band from 100-400 GHz with the constituents to be detected*

Constituents	**Frequencies**
100-200	CO, H_2O
200-300	CO
300-400	SO_2, HDO, CO, H_2O

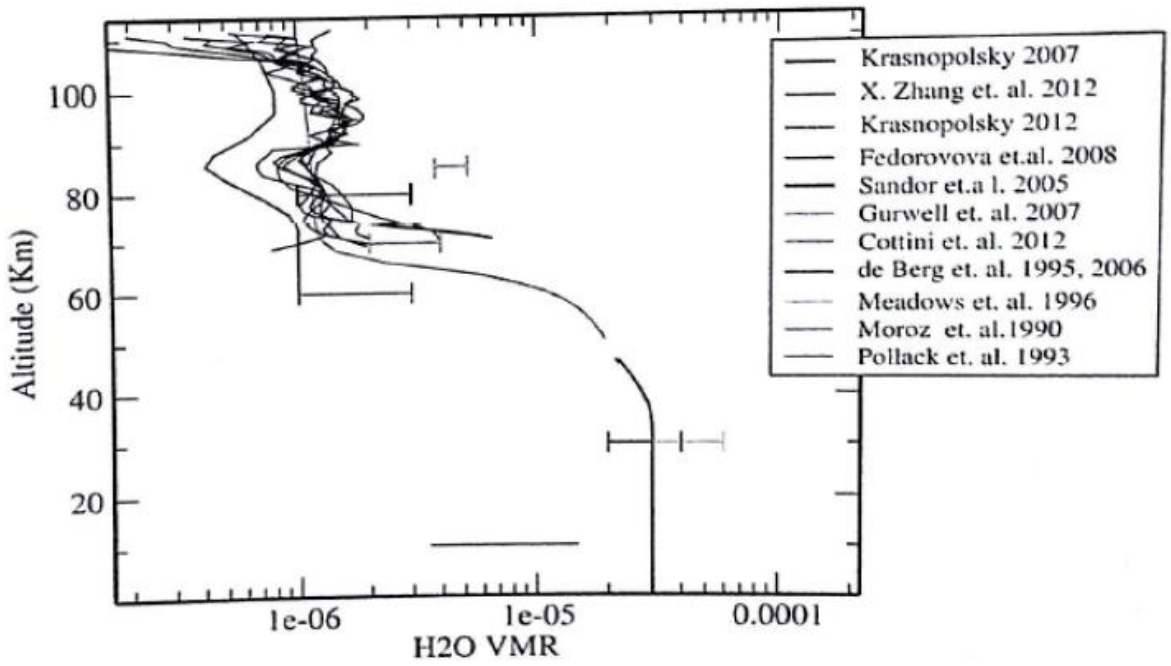

Figure 1. The water vapor information from various studies in the last few decades (both experimental and simulation) are show here. It is clear that there is high amount of uncertainty associated with the water vapor information from 60-100 km.

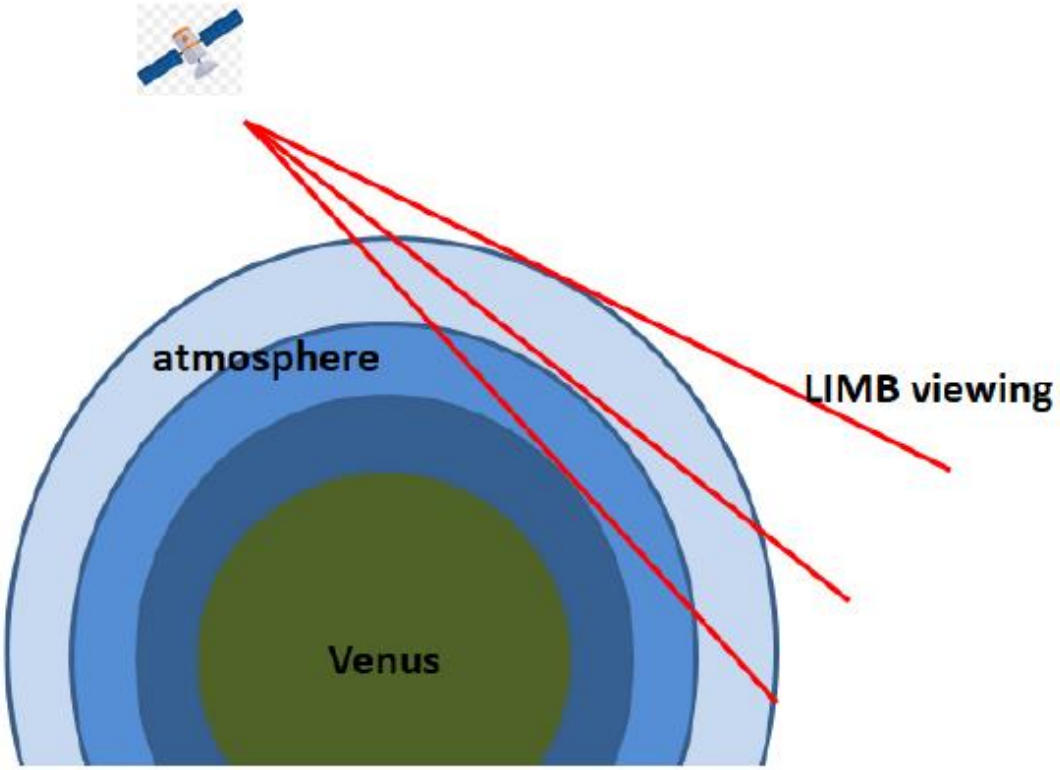

Figure 2. Instrument limb view with respect to Venus (used for the simulation) which can look through atmosphere at various altitudes.

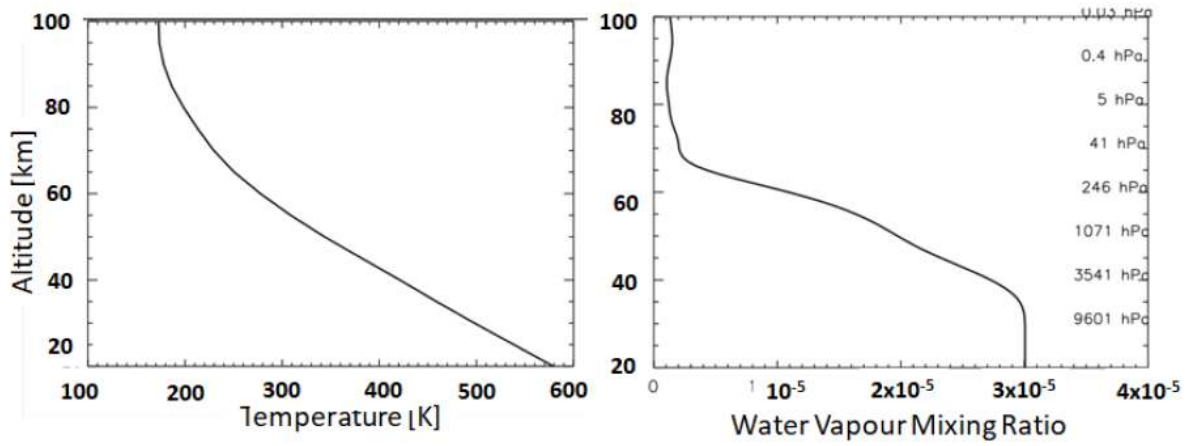

Figure 3. The night time Venus atmospheric (a) Temperature profile and (b) Water vapor mixing ratio profile.

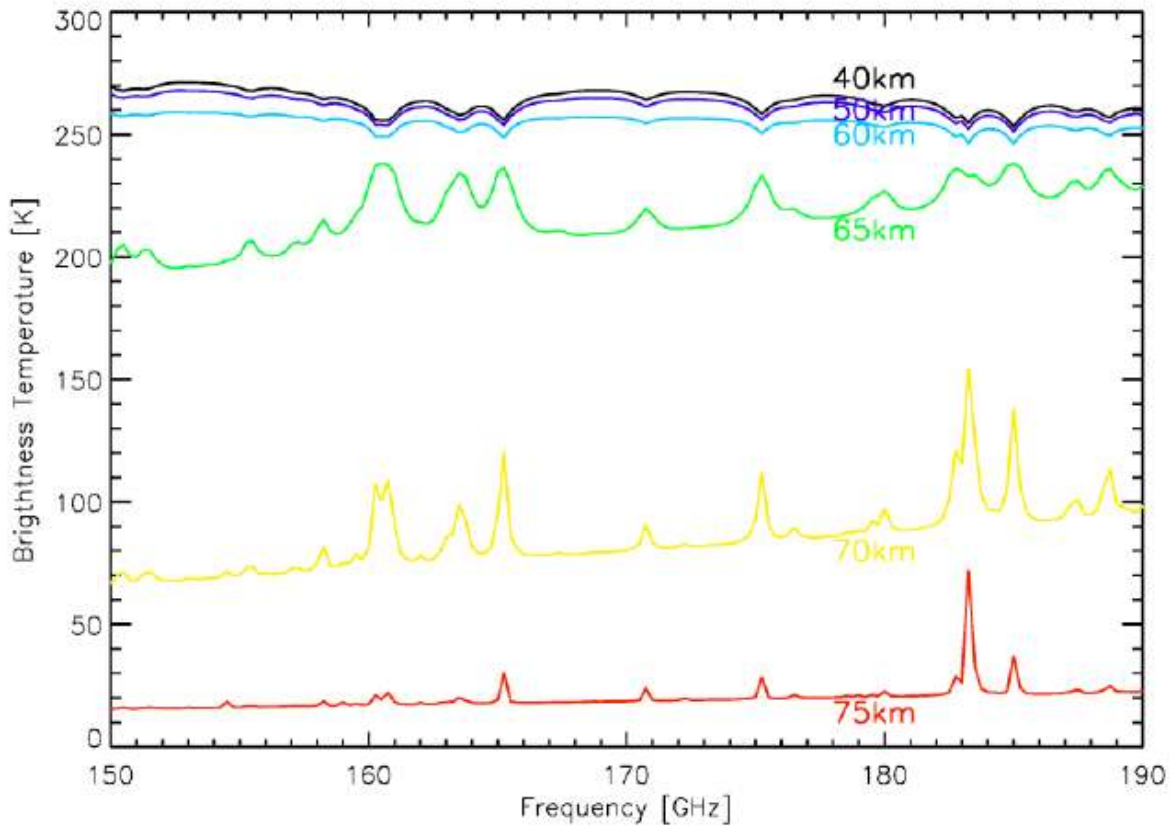

Figure 4. Brightness temperatures simulated from water vapor and temperature profiles during night time. The brightness temperature for radiometer viewing (limb) at various altitudes (40-75 km) above ground level is presented in various colors.

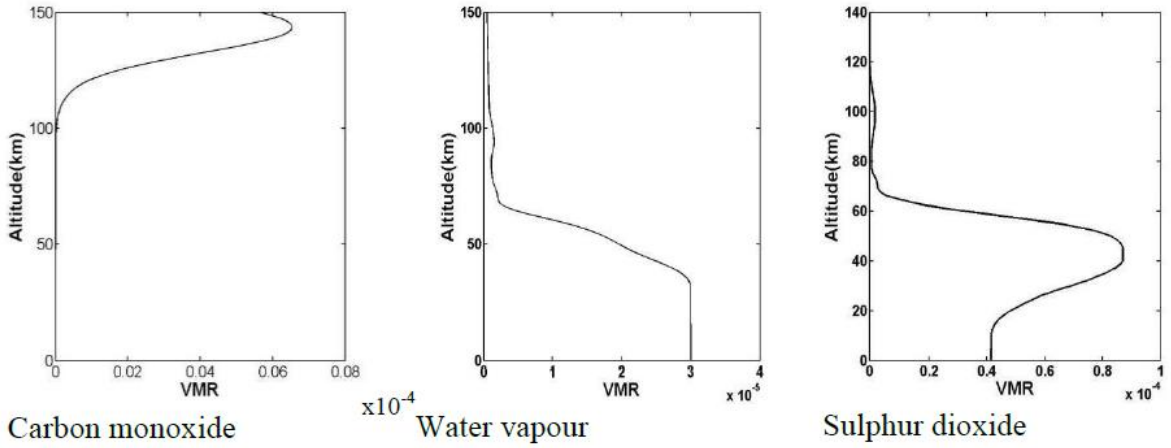

Figure 5. The volume mixing ratio profiles from ground level to altitude of 150 km for carbon monoxide, water vapor and sulphur dioxide.

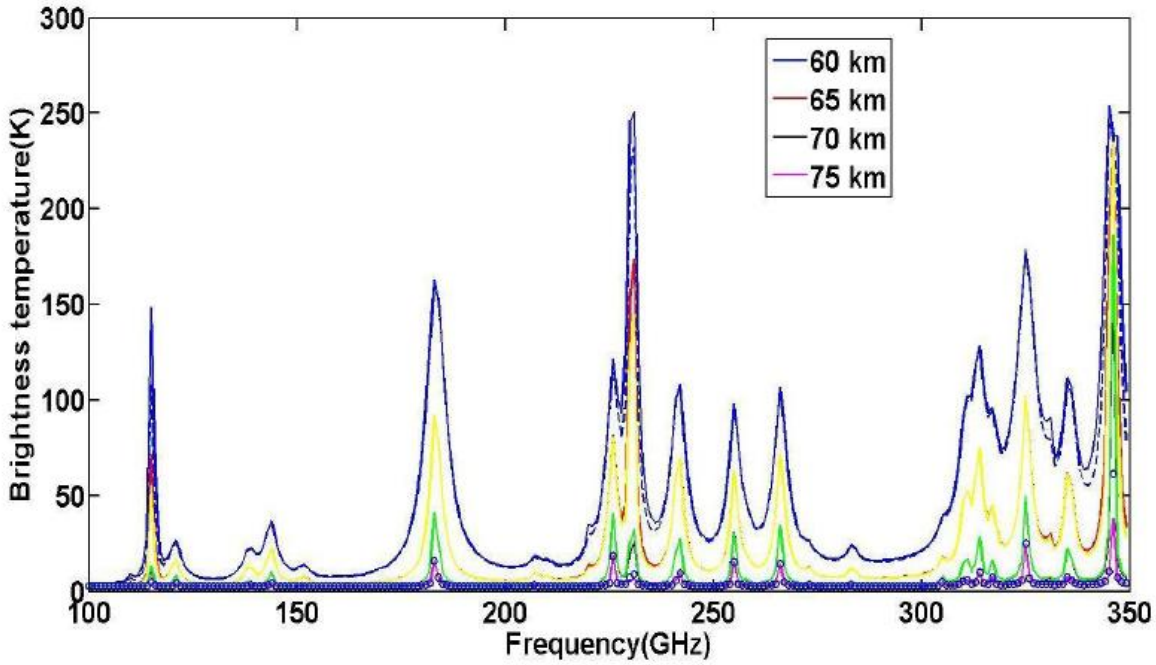

Figure 6. Brightness temperatures simulated for CO, H2O and HDO for 100-350 GHz. The brightness temperature for radiometer viewing (limb) at various altitudes (40-75 km) above ground level is presented in various colors.

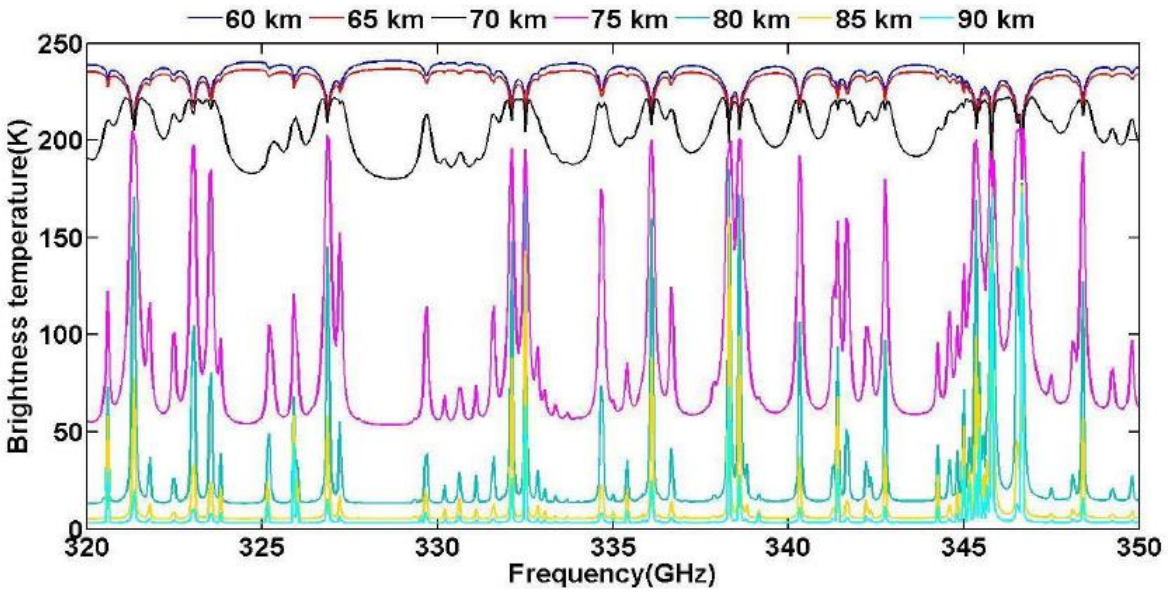

Figure 7. Brightness temperatures simulated for CO, HDO and SO_2 for 320-350 GHz. The brightness temperature for radiometer viewing (limb) at various altitudes (40-75 km) above ground level is presented in various colors.

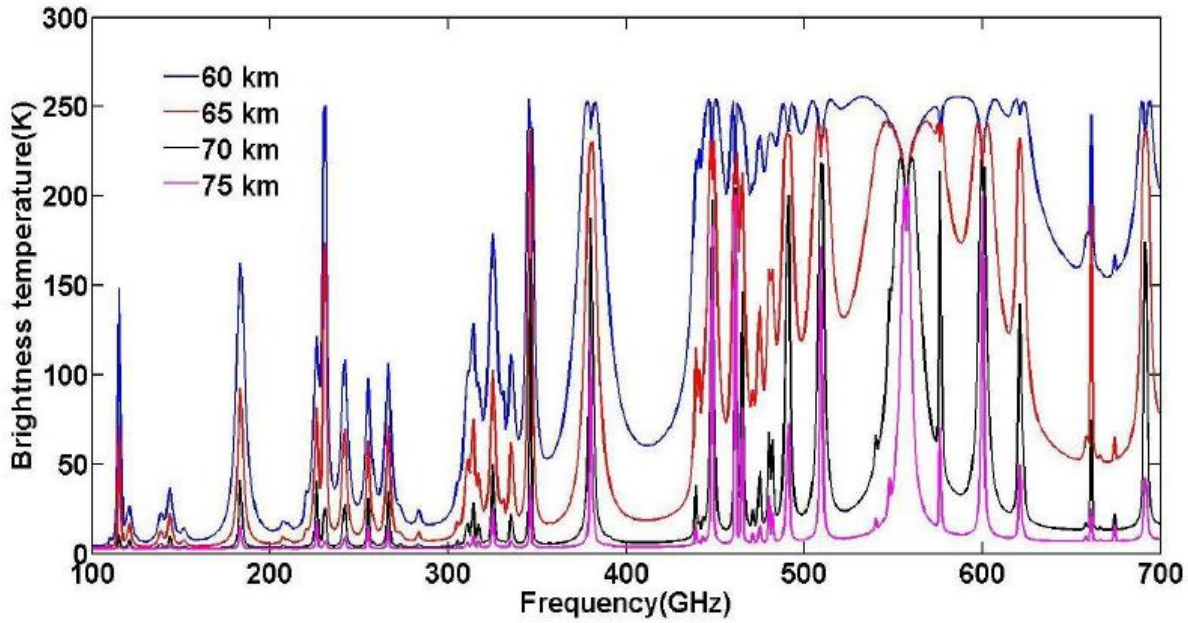

Figure 8. Brightness temperatures simulated for CO, H_2O, HCl, SO_2 and HDO for 100-700 GHz. The brightness temperature for radiometer viewing (limb) at various altitudes (40-75 km) above ground level is presented in various colors.

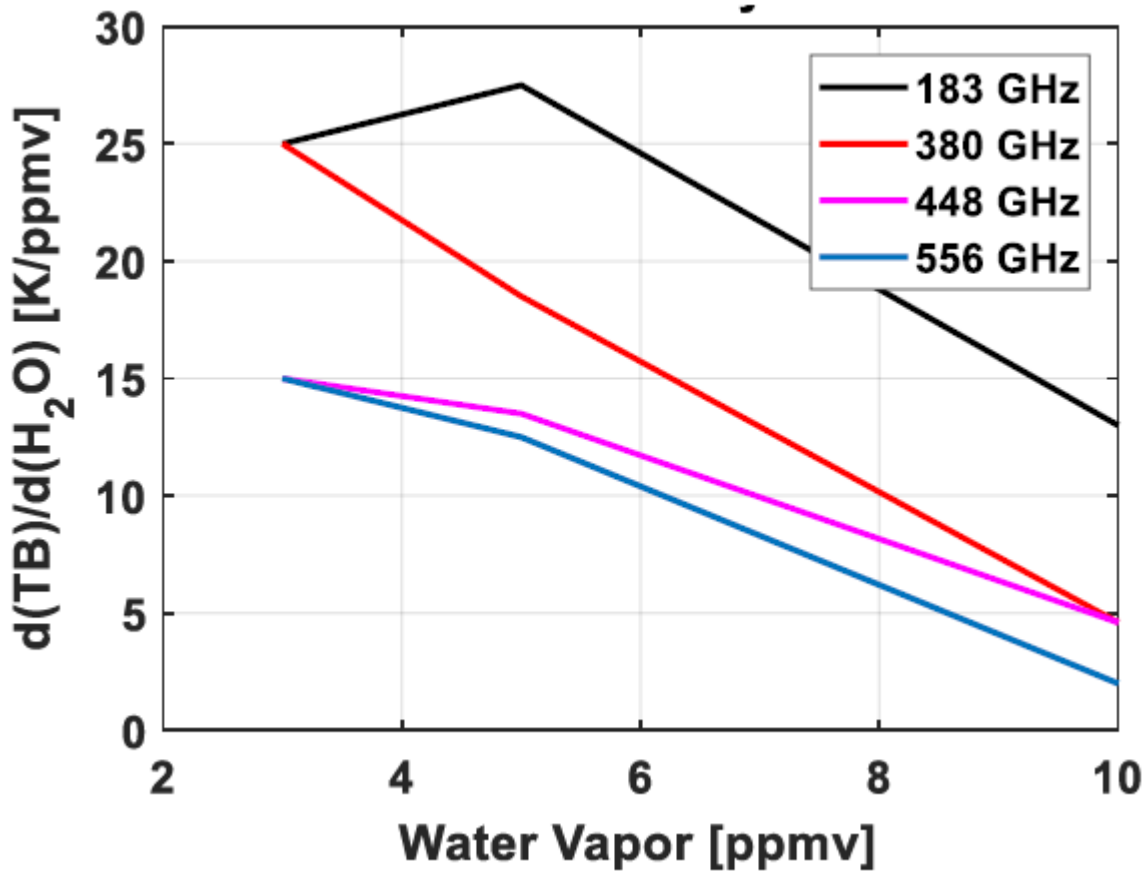

Figure 9. The rate of change of brightness temperatures for change in water vapor VMR for frequency channels 183, 380, 448, 556 GHz.

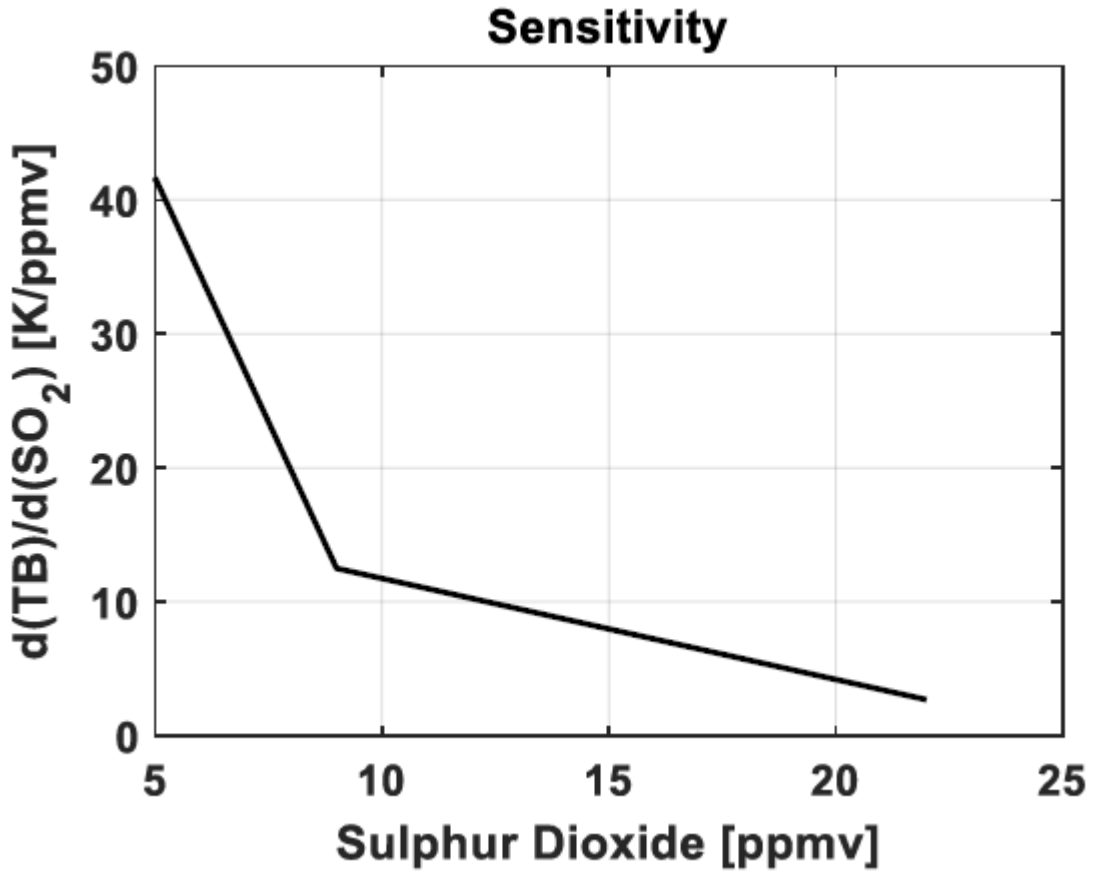

Figure 10. The rate of change of brightness temperatures for change in sulphur dioxide VMR for channel 346 GHz.